

Synthesis and characterization of a novel fluorene-based covalent triazine framework as a chemical adsorbent for highly efficient dye removal

Nazanin Mokhtari, Mohaddeseh Afshari, Mohammad Dinari^{*}

Department of Chemistry, Isfahan University of Technology, Isfahan, 84156-83111, Islamic Republic of Iran

ARTICLE INFO

Keywords:

Triazine-based covalent organic framework
Fluorene
Dye removal

ABSTRACT

Covalent organic frameworks (COFs) are known as emerging candidates for textile wastewater treatment due to their high porosity and regular channel structure. In the current paper, a Fluorene-based COF (FLU-COF) was synthesized by a facile method directing a crystalline framework. After a full characterization of the FLU-COF with different methods, its ability in removing Sky Blue A, widely used color in the textile industry, was investigated. Optimizing the parameters effective on the adsorption process by using the Central Composition Design, led to finding the optimal dye removal condition to be as pH 5; temperature: 45 °C; adsorbent dosage: 0.005 g; and contact time: 60 min. In this condition, the removal efficiency has reached over 99% with a maximum adsorption capacity of 299 mg. g⁻¹. The adsorption isotherm is consistent with the Langmuir model representing monolayer adsorption. Also, the kinetic investigations show the pseudo-second-order kinetics which means that the chemical interactions play an important role in dye removal. This is of important interest to make a laboratory method into an in-field method. Thus, a low-cost, simple, and portable method was introduced for investigation of the removal of Sky Blue A. In this regard, the ability of FLU-COF in removing dyes from aqueous solutions was examined by the mobile phone colorimetry as an alternative to the time-consuming laboratory methods. The comparison between the obtained results from mobile phone colorimetry and the traditional UV-Vis spectroscopy showed the accuracy of the method.

1. Introduction

Water pollution caused by accelerated development of industrialization, especially textile industries, has become the first global concern in recent years. Organic dyes are the most common pollutants in wastewaters. Azo dyes are one of the principal subdivisions of organic dyes that pose severe problems to human health [1]. Natural anaerobic degradation of azo compounds, and also other *N*-containing aromatics, form potentially carcinogenic aromatic amines [2,3]. Thus, removing these hazardous materials is necessarily required for the protection of human health and environmental [4]. In this regard, several conventional methods have been introduced, such as membrane filtration, photo-degradation, ion exchange, chemical oxidation, and adsorption. High efficiency, low process cost, and simplicity made adsorption the most favorable method [5].

Several porous materials with high surface areas including ordered mesoporous carbons, activated carbon (AC) [6,7], zeolites [8], metal-organic frameworks (MOFs) [9,10], porous organic polymers (POPs) [11,12], and functionalized mesoporous silica [13] have been reported

as the adsorbent for dye removal. Currently, AC is the most common adsorbent for dye removal from aqueous solutions. However, its applicability is faced with limitations due to the low adsorption capacity, slow adsorption kinetics, high cost, and difficult restoration. In order to address these problems, new porous materials such as MOFs have been proposed as high-performance adsorbents [14]. Although the use of MOFs due to their high adsorption capacity has attracted much attention in dye removal, their poor chemical stability and high sensitivity to moisture limit their practical application. New POPs by making strong covalent bonds between light elements have overcome this challenge and exhibiting high chemical and thermal stability under environmental conditions [15–18].

Covalent organic frameworks (COFs) are a class of POPs with crystalline ordered structure and defined pores [19,20]. COFs consist of covalently bonded light elements, such as C, N, H, O, and B, extended in regular frameworks [21]. Since their discovery in 2005, different linkages (e.g., hydrazine, imine, boroxine, and boronate) with different molecular geometry (e.g., hexagonal, kagome, and square) have been introduced [19,22]. A precise selection of linker and vertex could help

^{*} Corresponding author.

E-mail addresses: dinari@iut.ac.ir, mdinary@gmail.com (M. Dinari).

scientists to predict the size of the pores in the structure [23]. COFs' unique properties such as high surface area, as well as the structural diversity and physicochemical stability, led to receiving extensive attention during the last decade [24]. They have been applied in different branches of science ranging from catalysis and adsorption to drug delivery and energy storage [19,25–31]. Although COFs properties and features suggest potential advantages, few investigations have been conducted for dye adsorption from aqueous media [32].

Developing portable methods for on-site analysis has attracted significant attention in recent years. The sample-handling and contamination problems, as well as the high cost and time-consumption of in-laboratory methods, increase interest in using the mobile phone colorimetric methods [33,34]. Although the in-laboratory methods are more reliable, the simplicity, portability, and capability of mobile phone colorimetric methods in-field analysis make them good candidates for replacing conventional methods [35,36].

In this manuscript, a Fluorene-based COF (FLU-COF) was designed and synthesized using 4,4',4''-(1,3,5-triazine-2,4,6-triyl)tris(oxy)tribenzaldehyde (TOB) as the vertex point and 2,7-diaminofluorene (DAF) as the linker by a modified hydrothermal method. The prepared FLU-COF was used to efficiently remove the highly water-soluble color Sky blue A. This dye is the main color in the textile industry, leather and jeans coloring, and paper-making. In order to find the optimal parameters of dye removal, the central composite design (CCD) was performed. Then, a portable colorimetric platform was designed using a mobile phone. The comparison between the results obtained from the smart-phone and the UV–Vis spectrometer shows the reliability of the smart-phone results and the capability of using this platform in-field analysis.

2. Materials and methods

2.1. Reagents

2,7-Diaminofluorene (DAF), 2,4,6-trichloro-1,3,5-triazine (TCT), tetrabutylammonium bromide (TBAB), *p*-hydroxybenzaldehyde, and acetic acid (glacial) were purchased from Merck (Hohenbrunn, Germany) chemical company. All the other materials were obtained from Aldrich Chemical Co and used without further purification.

2.2. Preparation of 4,4',4''-(1,3,5-triazine-2,4,6-triyl)tris(oxy)tribenzaldehyde (TOB)

TOB was synthesized by a modified procedure according to the literature [37,38]. In a typical procedure, 50 mL aqueous solution of NaOH (0.04 mol, 1.6 g) and *p*-hydroxybenzaldehyde (0.04 mol, 4.88 g) were prepared. Then, another 50 mL solution of TCT (0.01 mol, 1.84 g) in dichloromethane containing TBAB (6.5×10^{-5} mol, 0.020 g) was prepared separately. These solutions were mixed to obtain a biphasic mixture, which is stirred for 24 h at room temperature. After sufficient time, the organic phase separated and was washed with NaOH (10% w/v) and distilled water. In the end, the organic phase was dried using anhydrous sodium sulfate and evaporation under reduced pressure to obtain a fluffy white product. The product was further purified by recrystallization in ethyl acetate. Yield (%) = 89; m.p. (°C) = 174; ¹HNMR (CDCl₃): 7.310 (d, 6H, J = 6.8 Hz), 7.903 (d, 6H, J = 6.8 Hz), 9.978 (s, 3H); elemental analysis for C₂₄H₁₅N₃O₆ (calcd./found): C 65.31/65.03, H 3.41/3.74, N 9.59/9.42, O 21.75/21.81.

2.3. Synthesis of fluorene-based COF (FLU-COF)

Although the sealed Pyrex-tube method was used to prepare FLU-COF earlier, the crystallinity of the product was not satisfactory. Herein, we present a modified hydrothermal method to prepare the FLU-COF with higher crystallinity. To prepare FLU-COF, TOB (0.6 mmol, 0.26 g) was added to 15 mL solution of *o*-dichlorobenzene/*n*-butanol (1:1 v/v)

containing DAF (0.4 mmol, 0.08 g). Then, sonication was conducted for 30 min to obtain a homogeneous suspension. Thereafter, 2 mL acetic acid (6 M) added to the mixture, and then the mixture autoclaved for seven days at 85 °C. Subsequently, the autoclave was cooled to room temperature and the product collected by centrifugation (6000 rpm, 10 min). In order to remove the oligomers and unreacted precursors, the precipitate washed three times with tetrahydrofuran (THF), acetone, dichloromethane, and ethyl acetate, respectively. Finally, the obtained precipitate was dried at 90 °C for 24 h under vacuum.

2.4. Characterization

The structure of FLU-COF was studied by thermogravimetric analysis (TGA), single-point BET specific surface area analysis, field-emission electron microscopy (FE-SEM), powdered X-ray diffraction (PXRD), and Fourier transform infrared (FT-IR) spectroscopy, as described in the Supporting Information (SI).

2.5. Adsorption experiments

Sky Blue A (Acid blue 9, C₃₇H₄₂N₄O₉S₃, MW: 787.90 g.mol⁻¹), an organic pigment with high water solubility (50 g.L⁻¹ in 90 °C) which is mainly used for wool, silk, and nylon dyeing and exist in industrial wastewaters, is considered as a practical candidate for adsorption. A stock solution of Sky Blue A (1000 ppm) was prepared by dissolving an appropriate amount of solid Sky Blue A in distilled water. Different solutions with concentration ranges from 1.5 to 120 ppm were prepared by simple dilution of the stock solution and then used for the calibration curve (Fig. S2) by measuring their absorbance at 637 nm. In a general batch experiment, 10 mg of FLU-COF were taken into 5 mL of dye solution with different initial concentrations. After sufficient time, the adsorbent was centrifuged (6000 rpm, 10 min), and the supernatant subjected to a UV–Vis spectrophotometer. The parameters useful on the adsorption, such as contact time, pH, and adsorbent dosage, were investigated entirely. According to spectroscopic data, the removal efficiency (R_e) and equilibrium adsorption capacity (q_e) can be calculated as follow:

$$\%R_e = \frac{(C_0 - C_e)}{C_0} \times 100 \quad (1)$$

$$q_e = \frac{V}{m} (C_0 - C_e) \times 100 \quad (2)$$

where C₀ (mg.L⁻¹) stands for the initial concentration, and C_e (mg.L⁻¹) is the concentration of Sky Blue A at the equilibrium. Moreover, V (L) is the solution volume, and m (g) is the mass of adsorbent.

All the kinetic models used in the manuscript were presented in detail in the supporting information.

2.6. Mobile phone colorimetric method

A mobile phone (HTC m8 eye), quartz cell, and a 10 W LED lamp was used to prepare a simple colorimeter platform to measure the dye concentration in solutions. The ratio of red, green, and blue color value in the sample image was examined using the *Color Grab* software (version 3.6.1). The software output shows a different value for each color. Thus, the following equation was used to calculate the color ratio (CR) for the samples [39]:

$$CR = \frac{\frac{R_s}{R_r} + \frac{G_s}{G_r} + \frac{B_s}{B_r}}{3} \quad (3)$$

where R_s, G_s, and B_s stand for the red, green, and blue color value of the sample, respectively. Also, R_r, G_r, and B_r are attributed to the red, green, and blue color value of the reference solution (distilled water), respectively. In this regard, the concentrate of stock solutions was ranged from

0.5 mg. L⁻¹ to 50 mg. L⁻¹ for finding the calibration curve (Fig. S4).

3. Results and discussion

3.1. Synthesis and characterization of FLU-COF

The TOB, a trialdehyde compound, was synthesized through a simple displacement reaction between TCT and *p*-hydroxybenzaldehyde in the presence of NaOH in a biphasic solution of dichloromethane and water. In the second step, FLU-COF was prepared by a reaction between TOB and DAF in hydrothermal conditions at 85 °C. The dark green product is found to be insoluble in usual organic solvents such as *N,N*-dimethylformamide (DMF), dimethyl sulfoxide (DMSO), acetonitrile, chloroform, acetone, and ethanol. FLU-COF was thoroughly characterized, and its ability to remove organic dyes from wastewaters was investigated (Scheme 1).

The FT-IR spectra of TOB, DAF, and FLU-COF were presented in Fig. 1. The presence of peaks at 2700-2830 cm⁻¹ is attributed to the vibration of aldehyde C-H in the TOB structure. Moreover, the band that appeared at 1699 cm⁻¹ is attributed to the C=O vibration. The phenolic C-O bond vibration appeared at 1211 cm⁻¹. The bands shown at 1372-1565 cm⁻¹ are attributed to the C-N and C=N bonds in the triazine ring (Fig. 1a). The presence of two bands at 3350-3410 cm⁻¹ is related to the amine group presented in the DAF (Fig. 1b) [40]. Evidence of the formation of FLU-COF is the disappearance of the C=O stretching frequency at 1699 cm⁻¹ and the formation of new imine bonds, which are presented at 1571 cm⁻¹ (Fig. 1c).

The X-ray diffraction pattern of FLU-COF is presented in Fig. 2(a). The diffraction peaks existed in 3.2°, and 5.8° were assigned to (1 0 0) and (2 1 0) plates, which are a result of the formation of hexagonal structure. The presence of (1 0 0) facet at 3.2° suggested that the FLU-COF can be in both eclipsed and staggered form. For a better comparison, the predicted XRD patterns of FLU-COF were shown in Fig. 2(b and c) [41].

The stability of the FLU-COF was investigated by using TGA (Fig. 3). The FLU-COF shows high thermal stability with a char yield of 57% (at

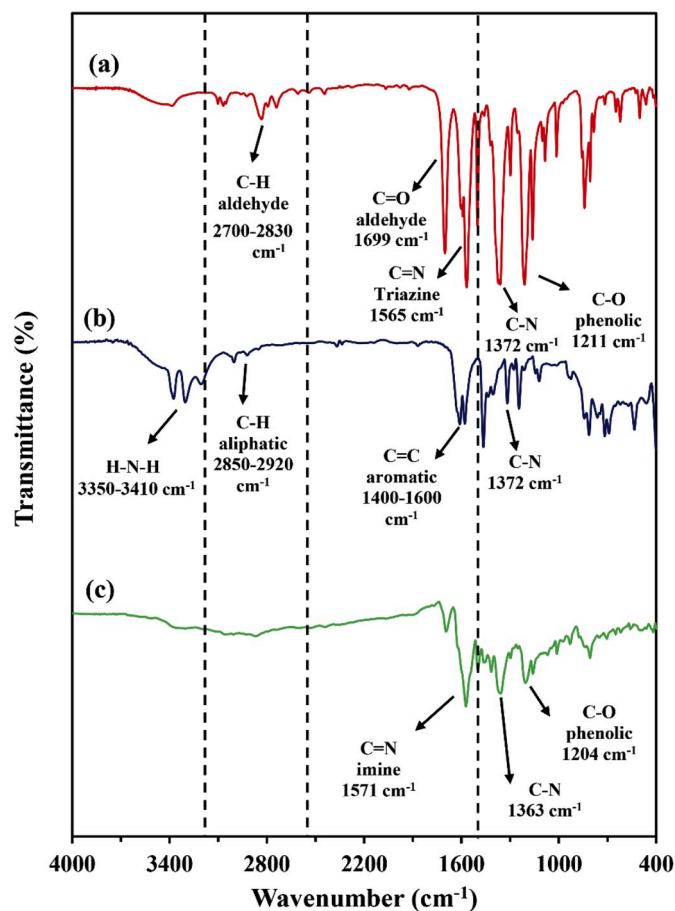
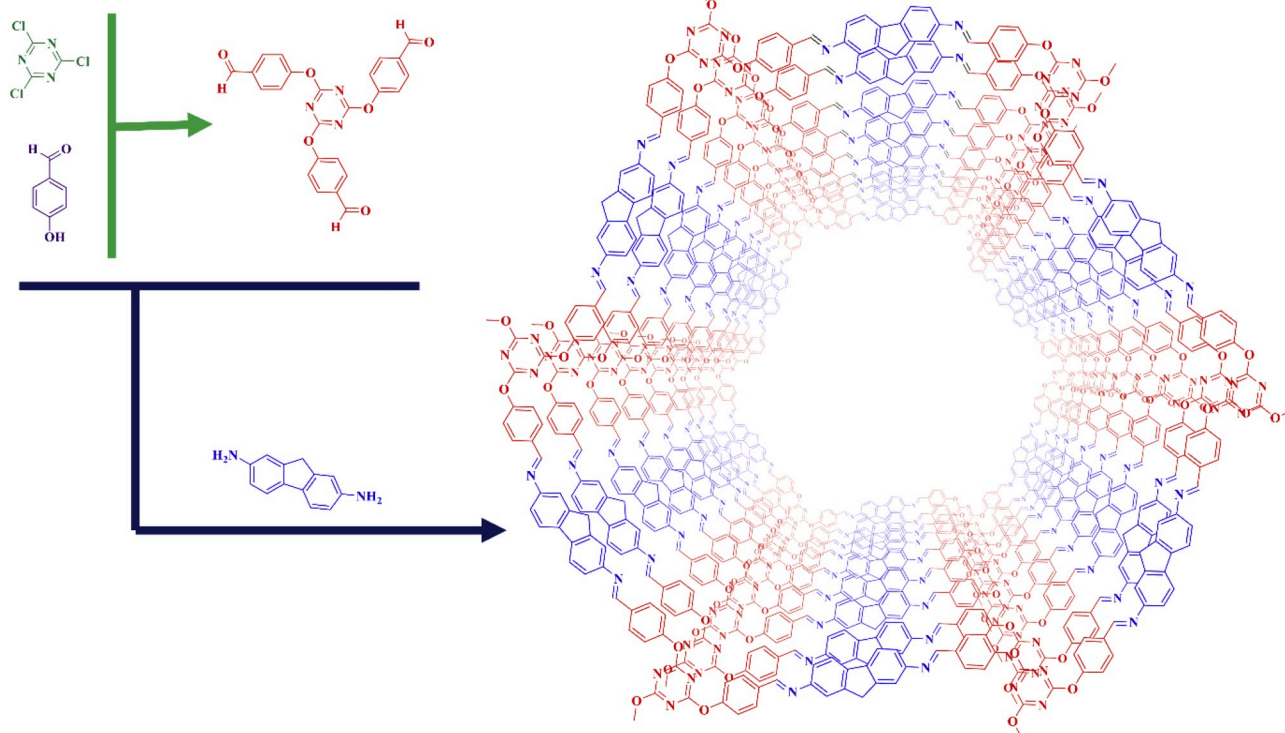


Fig. 1. FT-IR spectra of (a) TOB, (b) DAF, and (c) FLU-COF.



Scheme 1. Schematic view of the preparation of FLU-COF.

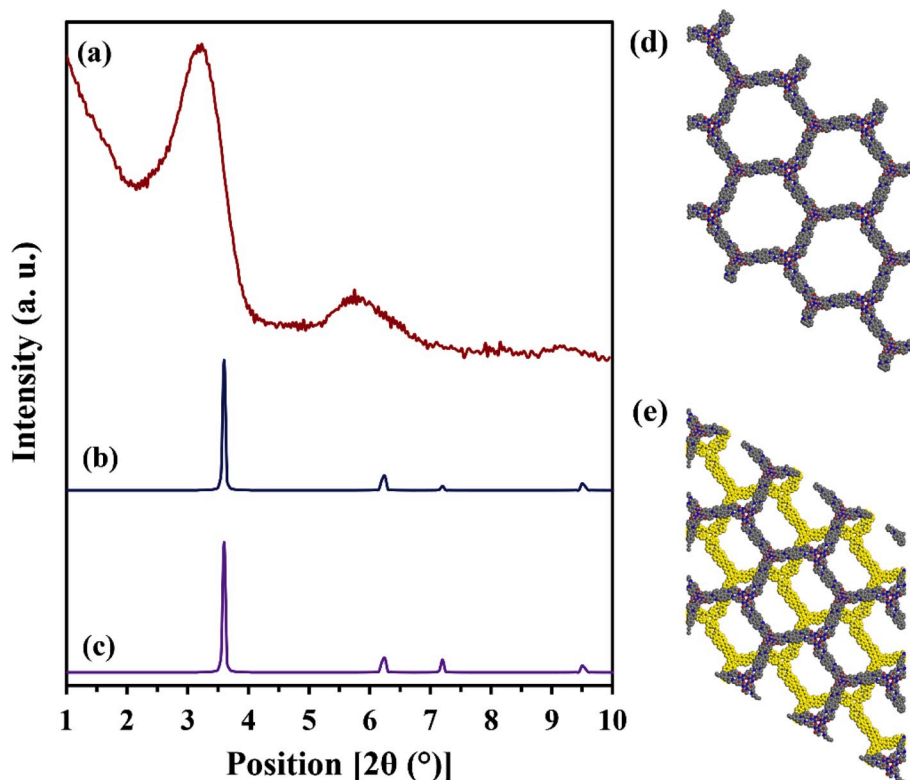


Fig. 2. XRD pattern of (a) FLU-COF, (b) predicted eclipsed form, (c) predicted staggered form, (d) eclipsed form of FLU-COF, and (e) staggered form of FLU-COF.

800 °C, Ar atmosphere). The physisorbed moisture led to a small mass loss below 100 °C. The decomposition temperature of 5% wt. (T5%) and 10% wt. (T10%) were 210 °C and 317 °C, respectively. Furthermore, in a halogen-free structure, there is a correlation between the char yield and the limiting oxygen index (LOI) described by Van Krevelen and Hoftzyer [42]. Thus, the LOI of FLU-COF is found to be 40.3. The data obtained from the TGA curve was summarized in Table 1. Hence, the FLU-COF can be classified in self-extinguishing material. The DTA also substantiates the results obtained from the TGA.

The surface morphology of the FLU-COF was investigated by FESEM, EDX, and elemental mapping. The FESEM images (Fig. 4a) exhibit a flake-like structure, in contrast to the amorphous structure presented by Konavrapu [43]. Moreover, the surface homogeneity was studied by elemental mapping analysis and EDX (Fig. 4b and c). The single point BET analysis showed a specific surface area of 264.6 m². g⁻¹.

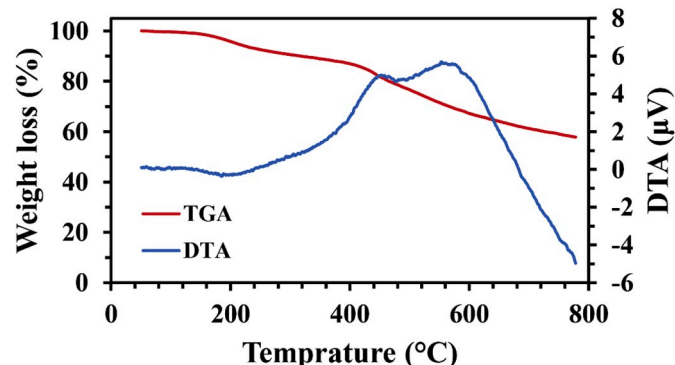


Fig. 3. TGA and DTA curve of FLU-COF.

Table 1
Thermal properties of the FLU-COF.

Samples	T _{dec} ^{0.5} (°C)	T _{dec} ¹⁰ (°C)	Char yield (%)	LOI (%)
FLU-COF	210	317	57	40.3

3.2. Dye adsorption

3.2.1. Optimization strategy

Optimization of adsorption condition is one of the critical steps to achieve the maximum adsorption capacity by FLU-COF. The effect of operating parameters, such as pH, temperature, contact time, and adsorbent dosage, should be investigated for optimization; one way is studying the effect of different values of each variable in invariant value for other variables that known as on factor at a time. Another way is the investigation of the relationship between variables specified by using statistical experimental design. In the design of the experiment method (DOE), a set of pre-designed experiments will be done [44]. The advantages of this method are reducing the test number, less consumption of time and material, finding the real optimize condition by the multi-variable interaction, and discover a mathematical model that shows the relation of the experiment parameter with test results [45].

In this study, the level of useful parameters was optimized by using the central composition design (CCD). The CCD consist of a fractional factorial design, a star design that can estimate the mathematical model includes constant and linear terms, interactions, and a quadratic term. The experiment was done in one block. The main parameter and their levels are shown in Table 2. The designed matrix and the experiment results are shown in Table 2.

3.2.2. ANOVA analysis and model fitting

The precision and accuracy of the designed method were examined using the analysis of variance method (ANOVA). The results are presented in Table S1. The result of ANOVA Interpretation and the model

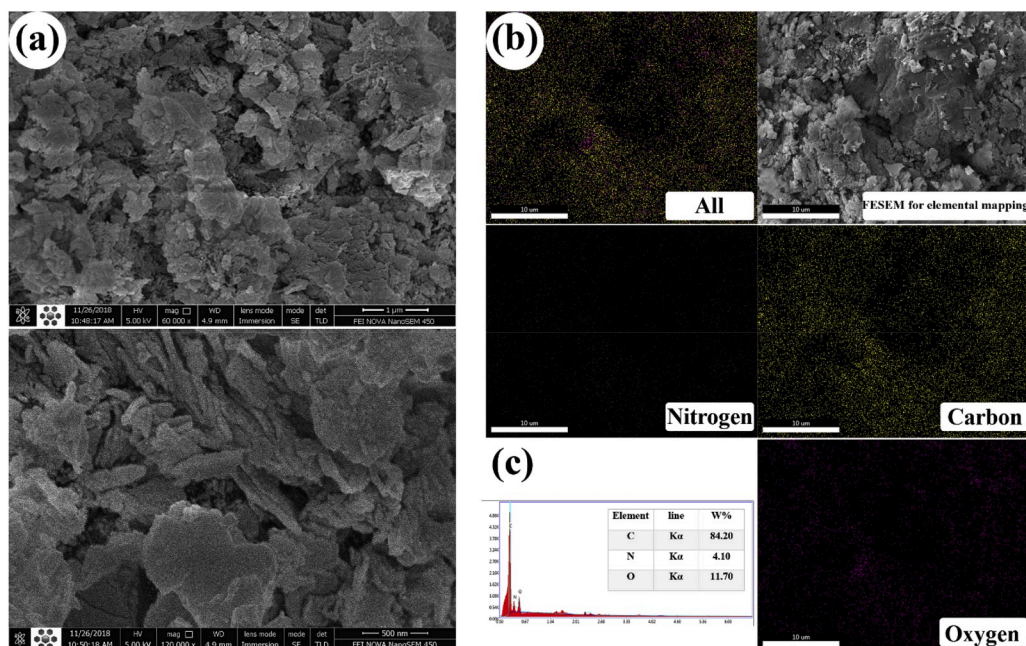


Fig. 4. (a) FESEM images of FLU-COF, (b) elemental mapping, and (c) EDX pattern of FLU-COF.

Table 2

Independent variables, their symbols, and levels for central composition design.

Variable	Effect symbol	Variable levels	
		-1	+1
Temperature (°C)	A	5	45
pH	B	3	9
Adsorbent Dosage (mg)	C	1.5	10
Time (min)	D	1	90

equation also presented in Supplementary material (Table S2). The F-value of the designed model found to be 12.70, representing that the model is significant. The probability of having a large F-value with this magnitude for a model by noise is only 0.01%.

Values of “Prob > F” less than 0.0500 indicate model terms are significant. In this case, B, C, D, C², D² are significant model terms. Values higher than 0.1000 indicate the model terms are not significant.

The “Lack of Fit F-value” of 2.63 implies the Lack of Fit is not significant relative to the pure error. There is a 14.85% chance that a “Lack of Fit F-value” this large could occur due to noise. Final Equation in Terms of Coded Factors is found to be as follow:

$$\text{Removal efficiency} = +89.24 + 2.06A - 3.87B + 13.41C + 3.65D - 3.03AB - 2.04AC - 0.60AD + 3.24BC - 0.39BD - 0.33CD + 1.96A^2 + 0.71B^2 - 5.90C^2 - 3.85D^2 \quad (4)$$

Here, Y is (%) of the color removal.

The influence of different factors such as contact time, pH, adsorbent dosage, and temperature on the removal efficiency was studied individually by using the CCD model, and their corresponding three-dimensional plots were shown in Fig. 5. The removal efficiency was increased by increasing the contact time until it reaches a maximum of 299.7 mg. g⁻¹. The removal efficiency insignificantly increased by temperature due to the endothermicity of the adsorption process. Regarding the results obtained from the CCD model, the optimal condition was found as contact time of 60 min; pH of 5; adsorbent dosage of 0.005 g, at 45 °C.

3.2.3. Adsorption at the equilibrium

The maximum value of the dye (mg) adsorbed per adsorbent mass

unit (g), can be calculated with the adsorption isotherms. According to the literature [5], the adsorption capacity (q_m) obtained from the adsorption isotherms can be used to indicate the adsorbent characteristics. Fig. 6a shows the adsorption isotherm of Sky Blue A over FLU-COF. The presence of aromatic rings and the formation of π-π stacking forces between the adsorbent and the Sky Blue A dye structure, as well as the presence of amine and imine functional groups and formation of hydrogen bonds between FLU-COF and dye molecules, lead to prepare an excellent condition for removing highly steric organic dye. Regarding this information, different isotherms (Langmuir, Freundlich, Temkin, and Dubinin-Radushkevich) [46] have been examined, and their results were summarized in Table .3 and Fig. S3. The intra-particle diffusion model was studied to gain more information about the adsorption process. A quick look at the Weber-Morris plot (Fig. S3 f) shows initial fast adsorption followed by a linear plateau. Thus, it could be said that the adsorption process consists of two steps. At first, the dye molecules were diffused through the solution to the external surface of FLU-COF indicating a mass transfer from the solution to the external surface of the adsorbent. In the second step, the adsorption-desorption process led to establishing an equilibrium which is shown in Fig. S3 f as a linear plateau [47–49]. Also, according to the correlation coefficient (R²), the adsorption data were best fitted to the Langmuir model corroborating the monolayer adsorption of Sky Blue A on the exterior surface of FLU-COF [50]. Thus, dye molecules were not penetrating into the inner layers of adsorbent. The adsorption energy emphasizes this point that completed adsorption is only obtained by the formation of a monolayer of adsorbate on the FLU-COF surface [51,52].

3.2.4. Adsorption kinetic study

To investigating the adsorption kinetics, the adsorption isotherm at optimal condition was fitted to the Elovich, Intra-particle diffusion, pseudo-first-order, and pseudo-second-order kinetic models. The results were summarized in Table 4, and the corresponding diagrams were presented in Fig. S3. The Pseudo-second-order model is most consistent with the experimental data, which means that the chemical interactions play an essential role in the Sky Blue A adsorption. According to the theory of classical physical chemistry, the adsorption is a surface effect that can be divided into physical adsorption and chemical adsorption. The kinetic studies show that the experimental data has followed the

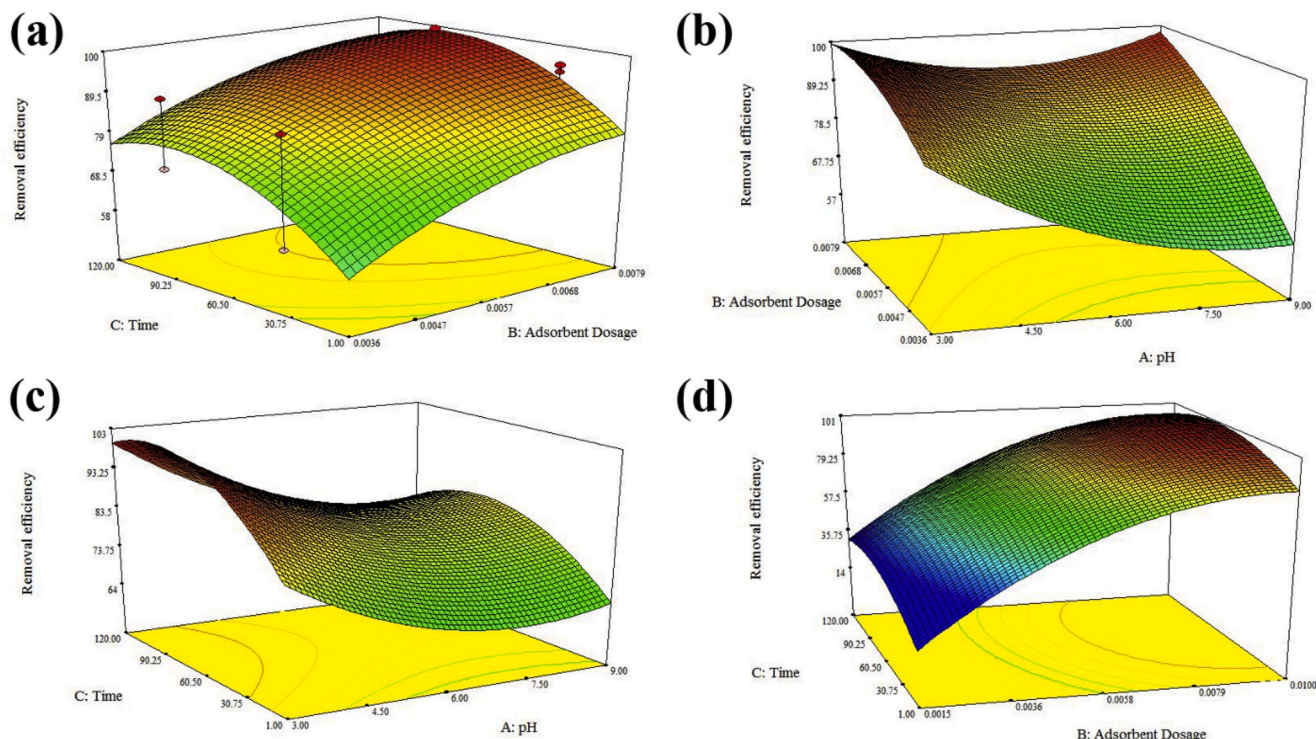


Fig. 5. Three dimensional (3d) plots of (a) contact time and adsorbent dosage, (b) adsorbent dosage and pH, (c) contact time and pH, and (d) contact time and adsorbent dosage.

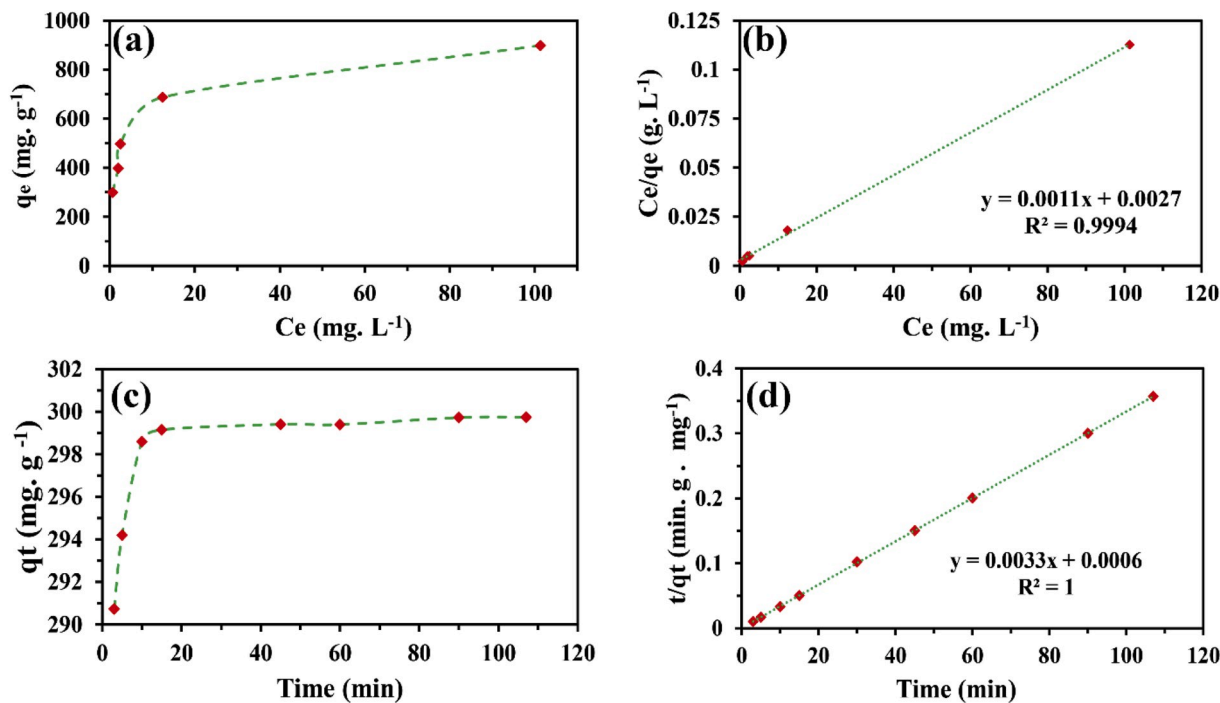


Fig. 6. (a) Adsorption isotherm for Sky Blue A over FLU-COF at optimal condition, (b) Langmuir plot of adsorption, (c) adsorption curve vs. contact time, and (d) pseudo-second-order kinetic model (condition: contact time of 60 min; pH of 5; adsorbent dosage of 0.005 g, at 45 °C). (For interpretation of the references to color in this figure legend, the reader is referred to the Web version of this article.)

pseudo-second-order model. Regarding the information in the literature [47,53,54], this model explains the presence of chemical interaction between the adsorbate and adsorbent. High nitrogen content of the FLU-COF with free lone pair electrons can cause the formation of hydrogen bonds between the adsorbent and the Sky Blue A. This process

can reach equilibrium by the formation of π - π stacking forces. There could be some interlayer hydrogen bonding forces in the FLU-COF, but the distance between the H-bonding donor and acceptor prevents the formation of intramolecular interactions (Scheme 1). According to previous studies [33,55], the presence of hydrogen bonding, would

Table 3

Isotherms coefficients for Sky Blue A adsorption over FLU-COF (condition: contact time of 60 min; pH of 5; adsorbent dosage of 0.005 g, at 45 °C).

Model	Langmuir			Freundlich			Temkin			Dubinin-Radushkevich		
	q _{max}	K _L	R ²	K _F	n	R ²	K _T	b _T	R ²	q _d	B	R ²
Sky Blue A	909	2.45	0.999	361.16	4.65	0.942	18.81	21.85	0.985	647.84	1.4·10 ⁻⁷	0.676

Table 4Kinetic coefficients for the adsorption of Sky Blue A by FLU-COF from its solutions (300 mg. L⁻¹, q_e exp.:299.74, condition: contact time of 60 min; pH of 5; adsorbent dosage of 0.005 g, at 45 °C).

Model	Pseudo- first order			Pseudo-second order			Intra-particle			Elovich		
	q _e	K ₁	R ²	q _e	K ₂	R ²	K _{id}	I	R ²	α	β	R ²
Sky Blue A	4.035	0.036	0.53	303.03	0.018	1	0.736	292.97	0.447	7.46·10 ⁶³	1.97	0.529

accelerate the adsorption process [56].

3.3. Mobile phone colorimetric method

To investigating the reliability of the method, adsorption isotherms and kinetic models were also studied and showed a complete consistency with the UV–Vis spectroscopy results (Figs. S5 and S6). Similarly, the Langmuir isotherm and the pseudo-second-order kinetic model were best fitted to the experimental data as it is summarized in Tables 5 and 6. Scheme 2 shows an illustration of the designed device for mobile phone colorimetry.

3.4. Comparison of FLU-COF adsorption capacity with recent studies on dye removal

The ability of FLU-COF in removing organic dyes was compared with recent studies and presented in Table 7. The impressive performance of FLU-COF within 60 min and adsorption capacity of 299 mg. g⁻¹ in comparison to MOFs (entries 1 and 3), and POPs (entry 2), and different nanocomposites (entries 4–8) corroborates the application of COFs in removing hazardous organic materials from water and wastewaters.

4. Conclusion

In conclusion, a fluorene-based covalent organic framework was synthesized following a condensation reaction between 4,4',4''-(1,3,5-triazine-2,4,6-triyl)tris(oxy)tribenzaldehyde and 2,7-diaminofluorene, and used for the adsorption of Sky Blue A from aqueous solutions. The maximum adsorption capacity of 299 mg. g⁻¹ was obtained, and its application on a mobile phone was investigated. The adsorption isotherm obeys the Langmuir equation representing monolayer adsorption, and the adsorption kinetic data follows the pseudo-second-order equation due to the presence of chemical interactions. The mobile phone colorimetric tests represent an excellent agreement with the experimental UV–Vis data. The ability of FLU-COF in colorimetry with portable devices can become an alternative to the conventional methods in field-analysis.

Funding

No funding was received for this work.

Table 5

Isotherms coefficients for Sky Blue A adsorption by smartphone colorimetric technique (condition: contact time of 90 min; pH of 5; adsorbent dosage of 0.005 g, at 45 °C).

Model	Langmuir			Freundlich			Temkin			Dubinin-Radushkevich		
	q _{max}	K _L	R ²	K _F	n	R ²	K _T	b _T	R ²	q _d	B	R ²
Sky Blue A	666	0.0021	0.972	0.018	2.07	0.949	18.81	16.81	0.97	437.95	5.2·10 ⁻³	0.913

Intellectual property

We confirm that we have given due consideration to the protection of intellectual property associated with this work and that there are no impediments to publication, including the timing of publication, with respect to intellectual property. In so doing we confirm that we have followed the regulations of our institutions concerning intellectual property.

Research ethics

We further confirm that any aspect of the work covered in this manuscript that has involved human patients has been conducted with the ethical approval of all relevant bodies and that such approvals are acknowledged within the manuscript.

IRB approval was obtained (required for studies and series of 3 or more cases)

Written consent to publish potentially identifying information, such as details or the case and photographs, was obtained from the patient(s) or their legal guardian(s).

We confirm that the manuscript has been read and approved by all named authors.

We confirm that the order of authors listed in the manuscript has been approved by all named authors.

Declaration of competing interest

No conflict of interest exists.

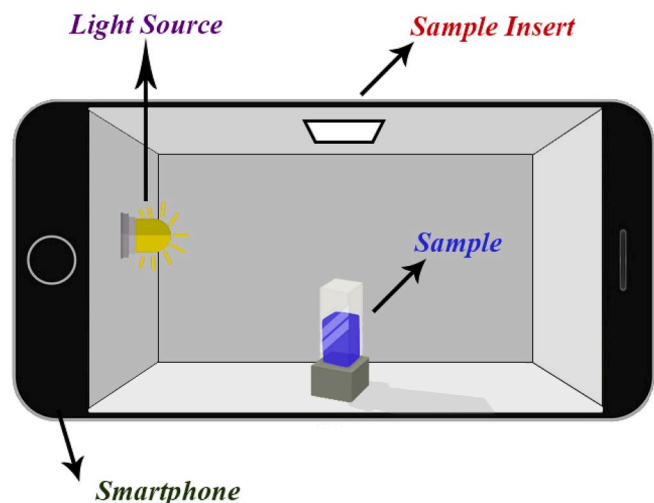
CRediT authorship contribution statement

Nazanin Mokhtari: Software, Visualization, Writing - original draft, Formal analysis, Investigation. **Mohaddeseh Afshari:** Software, Formal analysis, Writing - original draft. **Mohammad Dinari:** Supervision, Project administration, Conceptualization, Validation, Investigation, Resources, Writing - review & editing.

Table 6

Kinetic coefficients for the adsorption of Sky Blue A by smartphone colorimetric technique (condition: contact time of 90 min; pH of 5; adsorbent dosage of 0.005 g, at 45 °C).

Model	Pseudo- first order			Pseudo-second order			Intra-particle			Elovich		
	q _e	K ₁	R ²	q _e	K ₂	R ²	K _{id}	I	R ²	α	β	R ²
Sky Blue A	100.7	0.035	0.82	270.3	0.001	0.998	12.35	155.66	0.854	4.37	28.75	0.975



Scheme 2. Schematic view of smartphone colorimeter to estimate the dye concentration.

Table 7

A comparison of FLU-COF with recent adsorbents on dye removal.

Entry	Adsorbent	Adsorbate	C _i (mg. L ⁻¹) ^a	Time (min)	q _e (mg. L ⁻¹)	Reference
1	Zr-based MOF	Acid Blue 92	40	40	40.0	[57]
2	TPOP-SO ₃ H	Methylene blue	300	150	97.1	[58]
3	Cd-MOF1	Methylene blue	10	30	105.0	[59]
4	GO-Fe ₃ O ₄	Methylene blue	20	3	32.0	[60]
5	D-GO-COOH-(PEI-PAA) ₈	Methylene blue	10	120	43.9	[61]
6	PVA-PAA-GO-COOH-PDA	Congo red	25	240	9.6	[62]
7	PVA-PAA-GO-COOH-PDA	Methylene blue	10	240	26.9	[62]
8	Magnetic MWCNT	Methylene blue	3.74	360	11.9	[63]
9	FLU-COF	Sky Blue A	300	60	299.0	Present study

^a Initial concentration.

Appendix A. Supplementary data

Supplementary data to this article can be found online at <https://doi.org/10.1016/j.polymer.2020.122430>.

References

- Y. Zhang, G. Huang, C. An, X. Xin, X. Liu, M. Raman, Y. Yao, W. Wang, M. Doble, Transport of anionic azo dyes from aqueous solution to gemini surfactant-modified wheat bran: synchrotron infrared, molecular interaction and adsorption studies, *Sci. Total Environ.* 595 (2017) 723–732.
- D. Brown, P. Laboureur, The degradation of dyestuffs: part I primary biodegradation under anaerobic conditions, *Chemosphere* 12 (3) (1983) 397–404.
- J. McCann, E. Choi, E. Yamasaki, B.N. Ames, Detection of carcinogens as mutagens in the Salmonella/microsome test: assay of 300 chemicals, *Proc. Natl. Acad. Sci. Unit. States Am.* 72 (12) (1975) 5135–5139.
- S. Young, L. Balluz, J. Malilay, Natural and technologic hazardous material releases during and after natural disasters: a review, *Sci. Total Environ.* 322 (1–3) (2004) 3–20.
- B. Chen, X. Wang, C. Wang, W. Jiang, S. Li, Degradation of azo dye direct sky blue 5B by sonication combined with zero-valent iron, *Ultrason. Sonochem.* 18 (5) (2011) 1091–1096.
- A. Roghanizad, M.K. Abdolmaleki, S.M. Ghoreishi, M. Dinari, One-pot synthesis of functionalized mesoporous fibrous silica nanospheres for dye adsorption: isotherm, kinetic, and thermodynamic studies, *J. Mol. Liq.* 300 (2020), 112367.
- A.F. Streit, L.N. Cortes, S.P. Druzian, M. Godinho, G.C. Collazzo, D. Perondi, G. L. Dotto, Development of high quality activated carbon from biological sludge and its application for dyes removal from aqueous solutions, *Sci. Total Environ.* 660 (2019) 277–287.
- H. Mittal, R. Babu, A.A. Dabbawala, S. Stephen, S.M. Alhassan, Zeolite-Y incorporated karaya gum hydrogel composites for highly effective removal of cationic dyes, *Colloid. Surface. Physicochem. Eng. Aspect.* 586 (2020), 124161.
- M. Hasanzadeh, A. Simchi, H.S. Far, Nanoporous composites of activated carbon-metal organic frameworks for organic dye adsorption: synthesis, adsorption mechanism and kinetics studies, *J. Ind. Eng. Chem.* 81 (2020) 405–414.
- E. Wu, Y. Li, Q. Huang, Z. Yang, A. Wei, Q. Hu, Laccase immobilization on amino-functionalized magnetic metal organic framework for phenolic compound removal, *Chemosphere* 233 (2019) 327–335.
- M. Li, H. Zhao, Z.-Y. Lu, Porphyrin-based porous organic polymer, Py-POP, as a multifunctional platform for efficient selective adsorption and photocatalytic degradation of cationic dyes, *Microporous Mesoporous Mater.* 292 (2020), 109774.
- R. Soltani, A. Shahvar, H. Gordan, M. Dinari, M. Saraji, Covalent triazine framework-decorated phenyl-functionalised SBA-15: its synthesis and application as a novel nanoporous adsorbent, *New J. Chem.* 43 (2019) 13058–13067.
- W. Zhao, J. Sun, Q. Tang, H. Kong, Y. Fu, B. Jiang, Y. Zhang, Q. Ji, Atomic intercalation of magnesium in mesoporous silica hollow spheres and its effect for removal of dyes, *Appl. Surf. Sci.* 507 (2020), 144919.
- N.M. Mahmoodi, M. Oveisi, A. Panahdar, B. Hayati, K. Nasiri, Synthesis of porous metal-organic framework composite adsorbents and pollutant removal from multicomponent systems, *Mater. Chem. Phys.* 243 (2020), 122572.
- W. Gao, J. Tian, Y. Fang, T. Liu, X. Zhang, X. Xu, X. Zhang, Visible-light-driven photo-Fenton degradation of organic pollutants by a novel porphyrin-based porous organic polymer at neutral pH, *Chemosphere* 243 (2020), 125334.
- M. Huang, L. Yang, X. Li, G. Chang, An indole-derived porous organic polymer for efficiently visual colorimetric capture of iodine in aqueous media via the synergistic effects of cation- π and electrostatic forces, *Chem. Commun.* 56 (2020) 1401–1404.
- Z.-W. Liu, C.-X. Cao, B.-H. Han, A cationic porous organic polymer for high-capacity, fast, and selective capture of anionic pollutants, *J. Hazard Mater.* 367 (2019) 348–355.
- X. Zhang, J. Wang, X.-X. Dong, Y.-K. Lv, Functionalized metal-organic frameworks for photocatalytic degradation of organic pollutants in environment, *Chemosphere* (2019), 125144.
- S.-Y. Ding, W. Wang, Covalent organic frameworks (COFs): from design to applications, *Chem. Soc. Rev.* 42 (2) (2013) 548–568.
- A. Shahvar, R. Soltani, M. Saraji, M. Dinari, S. Aljani, Covalent triazine-based framework for micro solid-phase extraction of parabens, *J. Chromatogr. A* 1565 (2018) 48–56.
- A.P. Cote, A.I. Benin, N.W. Ockwig, M. O’Keeffe, A.J. Matzger, O.M. Yaghi, Porous, crystalline, covalent organic frameworks, *Science* 310 (5751) (2005) 1166–1170.
- S.D. Brucks, D.N. Bunck, W.R. Dichtel, Functionalization of 3D covalent organic frameworks using monofunctional boronic acids, *Polymer* 55 (1) (2014) 330–334.
- N. Huang, P. Wang, D. Jiang, Covalent organic frameworks: a materials platform for structural and functional designs, *Nat. Rev. Mater.* 1 (10) (2016) 1–19.
- M. Dinari, M. Hatami, Novel N-riched crystalline covalent organic framework as a highly porous adsorbent for effective cadmium removal, *J. Environ. Chem. Eng.* 7 (2019), 102907.
- J.W. Crowe, L.A. Baldwin, P.L. McGrier, Luminescent covalent organic frameworks containing a homogeneous and heterogeneous distribution of dehydrobenzoannulene vertex units, *J. Am. Chem. Soc.* 138 (32) (2016) 10120–10123.
- H. Furukawa, O.M. Yaghi, Storage of hydrogen, methane, and carbon dioxide in highly porous covalent organic frameworks for clean energy applications, *J. Am. Chem. Soc.* 131 (25) (2009) 8875–8883.

- [27] N. Mokhtari, S. Taymouri, M. Mirian, M. Dinari, Covalent triazine-based polyimine framework as a biocompatible pH-dependent sustained-release nanocarrier for sorafenib: an in vitro approach, *J. Mol. Liq.* 297 (2020), 111898.
- [28] L. Valentino, M. Matsumoto, W.R. Dichtel, B.J. Mariñas, Development and performance characterization of a polyimine covalent organic framework thin-film composite nanofiltration membrane, *Environ. Sci. Technol.* 51 (24) (2017) 14352–14359.
- [29] Y. Zeng, R. Zou, Y. Zhao, Covalent organic frameworks for CO₂ capture, *Adv. Mater.* 28 (15) (2016) 2855–2873.
- [30] M. Dinari, N. Mokhtari, S. Taymouri, M. Arshadi, A. Abbaspourrad, Covalent polybenzimidazole-based triazine frameworks: a robust carrier for non-steroidal anti-inflammatory drugs, *Mater. Sci. Eng. C* 108 (2020), 110482.
- [31] S. Gopi, M. Kathiresan, 1, 4-Phenylenediamine based covalent triazine framework as an electro catalyst, *Polymer* 109 (2017) 315–320.
- [32] S.-B. Yu, H. Lyu, J. Tian, H. Wang, D.-W. Zhang, Y. Liu, Z.-T. Li, A polycationic covalent organic framework: a robust adsorbent for anionic dye pollutants, *Polym. Chem.* 7 (20) (2016) 3392–3397.
- [33] M. Afshari, M. Dinari, Synthesis of new imine-linked covalent organic framework as high efficient adsorbent and monitoring the removal of direct fast scarlet 4BS textile dye based on mobile phone colorimetric platform, *J. Hazard Mater.* 385 (2020), 121514.
- [34] T.-S. Lai, T.-C. Chang, S.-C. Wang, Gold nanoparticle-based colorimetric methods to determine protein contents in artificial urine using membrane micro-concentrators and mobile phone camera, *Sensor. Actuator. B Chem.* 239 (2017) 9–16.
- [35] N.J. Vickers, Animal communication: when I'm calling you, will you answer too? *Curr. Biol.* 27 (14) (2017) R713–R715.
- [36] A. Shahvar, M. Saraji, D. Shamsaei, Headspace single drop microextraction combined with mobile phone-based on-drop sensing for the determination of formaldehyde, *Sensor. Actuator. B Chem.* 273 (2018) 1474–1478.
- [37] F.G. Khan, M.V. Yadav, A.D. Sagar, Synthesis, characterization, and antimicrobial evaluation of novel trichalcones containing core s-triazine moiety, *Med. Chem. Res.* 23 (5) (2014) 2633–2638.
- [38] N. Mokhtari, M.M. Khataei, M. Dinari, B.H. Monjezi, Y. Yamini, Imine-based covalent triazine framework: synthesis, characterization, and evaluation its adsorption, *Mater. Lett.* (2019), 127221.
- [39] S. Sumriddetchkajorn, K. Chaitavon, Y. Intaravanne, Mobile device-based self-referencing colorimeter for monitoring chlorine concentration in water, *Sensor. Actuator. B Chem.* 182 (2013) 592–597.
- [40] N. Mokhtari, M. Dinari, O. Rahmadian, Novel porous organic triazine-based polyimide with high nitrogen levels for highly efficient removal of Ni (II) from aqueous solution, *Polym. Int.* 68 (6) (2019) 1178–1185.
- [41] T. Ma, E.A. Kapustin, S.X. Yin, L. Liang, Z. Zhou, J. Niu, L.-H. Li, Y. Wang, J. Su, J. Li, Single-crystal x-ray diffraction structures of covalent organic frameworks, *Science* 361 (6397) (2018) 48–52.
- [42] P.J. Hoftyzer, D. Van Krevelen, Properties of Polymers: Correlations with Chemical Structure, Elsevier, Amsterdam, 1972.
- [43] S.K. Konavrapu, K. Biradha, Luminescent triazine-based covalent organic frameworks functionalized with imine and azine: N₂ and H₂ sorption and efficient removal of organic dye pollutants, *Cryst. Growth Des.* 19 (1) (2018) 362–368.
- [44] L. Mousavi, Z. Tamiji, M.R. Khoshayand, Applications and opportunities of experimental design for the dispersive liquid–liquid microextraction method—A review, *Talanta* 190 (2018) 335–356.
- [45] R. Leardi, Experimental design in chemistry: a tutorial, *Anal. Chim. Acta* 652 (1–2) (2009) 161–172.
- [46] M. Faraj, M. Erhayem, Langmuir, Freundlich, Temkin and dubinin–radushkevich isotherm studies of equilibrium sorption of methylene blue from aqueous solution onto mulberry tree (*morus nigra* L) roots powder, *J. Pure Appl. Sci. (Ankara)* 17 (1) (2018).
- [47] H.A. Ahsaine, M. Zbair, Z. Anfar, Y. Naciri, N. El Alem, M. Ezahri, Cationic dyes adsorption onto high surface area 'almond shell' activated carbon: kinetics, equilibrium isotherms and surface statistical modeling, *Mater. Today Chem.* 8 (2018) 121–132.
- [48] H.A. Ahsaine, M. Zbair, R. El Haouti, Mesoporous treated sewage sludge as outstanding low-cost adsorbent for cadmium removal, *Desalination Water Treat.* 85 (2017) 330–338.
- [49] S. Aoudj, A. Khelifa, N. Drouiche, R. Belkada, D. Miroud, Simultaneous removal of chromium (VI) and fluoride by electrocoagulation–electroflotation: application of a hybrid Fe-Al anode, *Chem. Eng. J.* 267 (2015) 153–162.
- [50] S. Sun, C. Wang, S. Han, T. Jiao, R. Wang, J. Yin, Q. Li, Y. Wang, L. Geng, X. Yu, Interfacial nanostructures and acidochromism behaviors in self-assembled terpyridine derivatives Langmuir-Blodgett films, *Colloid. Surface. Physicochem. Eng. Aspect.* 564 (2019) 1–9.
- [51] H. Baseri, S. Tizro, Treatment of nickel ions from contaminated water by magnetite based nanocomposite adsorbents: effects of thermodynamic and kinetic parameters and modeling with Langmuir and Freundlich isotherms, *Process Saf. Environ. Protect.* 109 (2017) 465–477.
- [52] C.S. Araújo, L.L. Almeida, H.C. Rezende, S.M. Marcionilio, J.J. Léon, T.N. de Matos, Elucidation of mechanism involved in adsorption of Pb (II) onto lobeira fruit (*Solanum lycocarpum*) using Langmuir, Freundlich and Temkin isotherms, *Microchem. J.* 137 (2018) 348–354.
- [53] H. Han, W. Wei, Z. Jiang, J. Lu, J. Zhu, J. Xie, Removal of cationic dyes from aqueous solution by adsorption onto hydrophobic/hydrophilic silica aerogel, *Colloid. Surface. Physicochem. Eng. Aspect.* 509 (2016) 539–549.
- [54] A. Maleki, U. Hamesadeghi, H. Daraei, B. Hayati, F. Najafi, G. McKay, R. Rezaee, Amine functionalized multi-walled carbon nanotubes: single and binary systems for high capacity dye removal, *Chem. Eng. J.* 313 (2017) 826–835.
- [55] X. Zhu, S. An, Y. Liu, J. Hu, H. Liu, C. Tian, S. Dai, X. Yang, H. Wang, C.W. Abney, Efficient removal of organic dye pollutants using covalent organic frameworks, *AIChE J.* 63 (8) (2017) 3470–3478.
- [56] C. Muthukumar, V.M. Sivakumar, M. Thirumarimurugan, Adsorption isotherms and kinetic studies of crystal violet dye removal from aqueous solution using surfactant modified magnetic nanoadsorbent, *J. Taiwan Inst. Chem. Eng.* 63 (2016) 354–362.
- [57] M. Hasanzadeh, A. Simchi, H.S. Far, Kinetics and adsorptive study of organic dye removal using water-stable nanoscale metal organic frameworks, *Mater. Chem. Phys.* 233 (2019) 267–275.
- [58] Y. Li, H. Wang, W. Zhao, X. Wang, Y. Shi, H. Fan, H. Sun, L. Tan, Facile synthesis of a triptycene-based porous organic polymer with a high efficiency and recyclable adsorption for organic dyes, *J. Appl. Polym. Sci.* 136 (39) (2019), 47987.
- [59] F.Y. Yi, J.P. Li, D. Wu, Z.M. Sun, A series of multifunctional metal–organic frameworks showing excellent luminescent sensing, sensitization, and adsorbent abilities, *Chem. Eur. J.* 21 (32) (2015) 11475–11482.
- [60] T. Jiao, Y. Liu, Y. Wu, Q. Zhang, X. Yan, F. Gao, A.J. Bauer, J. Liu, T. Zeng, B. Li, Facile and scalable preparation of graphene oxide-based magnetic hybrids for fast and highly efficient removal of organic dyes, *Sci. Rep.* 5 (2015), 12451.
- [61] X. Zhao, K. Ma, T. Jiao, R. Xing, X. Ma, J. Hu, H. Huang, L. Zhang, X. Yan, Fabrication of hierarchical layer-by-layer assembled diamond-based core-shell nanocomposites as highly efficient dye adsorbents for wastewater treatment, *Sci. Rep.* 7 (2017), 44076.
- [62] R. Xing, W. Wang, T. Jiao, K. Ma, Q. Zhang, W. Hong, H. Qiu, J. Zhou, L. Zhang, Q. Peng, Bioinspired polydopamine sheathed nanofibers containing carboxylate graphene oxide nanosheet for high-efficient dyes scavenger, *ACS Sustain. Chem. Eng.* 5 (6) (2017) 4948–4956.
- [63] J.-L. Gong, B. Wang, G.-M. Zeng, C.-P. Yang, C.-G. Niu, Q.-Y. Niu, W.-J. Zhou, Y. Liang, Removal of cationic dyes from aqueous solution using magnetic multi-wall carbon nanotube nanocomposite as adsorbent, *J. Hazard Mater.* 164 (2–3) (2009) 1517–1522.